Transactions of the TSME (2019) Vol. 7, No. 1, 83-90
Journal of Research and Applications in Mechanical Engineering

ISSN 2229-2152 print
DOI: 10.14456/jrame.2019.8

Research Article

ANODIC COATING OF MG-ND-GD-ZN-ZR (EV31A) AND MG-Y-ND-GD-ZR (WE43C) IN SALINE SOLUTION

N. Jakraphan[1],*
K.S. Raja[2]
[1] Department of Marine Engineering, Education Branch, Royal Thai Naval Academy, 204 Sukumwit Rd. Pak Num, Muang Samut Prakan, Samut Prakan, 10270
[2] Department of Chemical and Materials Engineering, University of Idaho, Moscow, Idaho, 83844, USA

Received 10 April 2019
Revised 5 June 2019
Accepted 7 June 2019

ABSTRACT:
Mg-Nd-Gd-Zn-Zr (EV31A) and Mg-Y-Nd-Gd-Zr (WE43C) are heat-treatable magnesium (Mg) alloys which are used in aerospace and high-performance applications. Their strength to weight ratios are higher than aluminum alloys. In addition, their corrosion resistance was improved. Anodization in NaF is a typical method to protect surface of Mg alloys from corrosion. EV31A and WE43C in as-received and peak-aged conditions were anodized in NaF and investigated. The studies were conducted in 0.1 M NaOH solution with 500 ppm of chloride concentration. Anodized EV31A in as-received condition showed similar pitting protection potential to the non-anodized one. In contrast, peak-aged EV31A which was not anodized presented better pitting protection potential compared to anodized peak-aged EV31A. Pitting protection potentials of both as-received and peak-aged conditions of WE43C were improved when the materials were anodized.

Keywords: *Magnesium rare earth alloy, Anodic coating, Chloride*

1. INTRODUCTION

Mg alloys are used in the applications which require light weight and good mechanical properties. Their relative densities approximate 1.8. In addition, their tensile strength may reach 325 MPa for high strength Mg alloys. Mg alloys show good corrosion resistance at pH around 9 and above because of their stable passive film. However, their corrosion resistance decrease when they are in chloride, sulfate, and sulfite solutions. As a result, anodic coating plays an important role in protecting Mg alloys' surface. Many anodizing methods are applied on Mg alloys such as DOW 17, HAE, and Keronite [1]. However, many new methods are investigated. Liyuan and co-workers [2] investigated AZ31 Mg alloy which was anodized in alkaline solutions with silicate. They found that AZ31 anodized in sodium silicate ($NaSiO_3$) showed best corrosion resistance compared to sodium aluminate ($NaAlO_2$) sodium phosphate (Na_3PO_4), and sodium molybdate (Na_2MoO_4). In addition, concentration of $NaSiO_3$ affected structure of anodic film. Corrosion resistance increased when concentration increased up to 90 g/l, then corrosion resistance decreased. Applied current density was also affected corrosion resistance of anodic film. High applied current density improved corrosion resistance of anodic film. Wu and co-workers [3] anodized AZ31 magnesium alloys in alkaline borate solutions with organic additive. They found that this additive helped the traditional additives to form ivory white smooth anodic film of AZ31 which improved corrosion resistance. Anodizing voltage, time, and additives were also affected the anodic film.

* Corresponding author: N. Jakraphan
E-mail address: palm_kalin@hotmail.com

2. EXPERIMENTAL METHOD

Mg-Nd-Gd-Zn-Zr (EV31A) and Mg-Y-Nd-Gd-Zr (WE43C) plates provided by Magnesium Elektron N.A. Inc. were cut into 1.5 cm × 2.5 cm × 0.3 cm coupons. The EV31A in peak-aged condition (PA) was solution heat-treated at 525°C for 8 h, quenched in room temperature water, and aged at 200°C for 16 h. The WE43C in peak-aged condition (PA) was solution heat-treated at 525°C for 8 h, quenched in room-temperature water, and aged at 250°C for 8 h. The as-received (AR) samples of both EV31A and WE43C were not done any additional heat treatment. Before doing anodic coating, all samples were polished with SiC paper down to 1500 grit, rinsed with ethanol and dried in air. The anodic coating was carried out in 1 M NaF at 60 V DC for 1 h. The optical microscopy was conducted by using OLYMPUS PMG3 optical microscope, and the FESEM: LEO SUPRA 35VP scanning electron microscope (SEM) was used in electron microscopy.

The electrochemical tests were conducted in PTFE electrochemical cell with 1 cm^2 exposed surface area. The sample was the working electrode, a platinum wire was used as a counter electrode, and Ag/AgCl was used as a reference electrode (199 mV vs SHE). The saline solution used in the experiment was 0.1 M NaOH (pH 13) with 500 ppm chloride concentration. Deionized water and laboratory grade chemicals were used in solution preparation. The cyclic polarization was conducted by scanning the potential from 0 V vs open circuit potential (OCP) to 2.5 V vs Ag/AgCl reference electrode. The scan direction went back to OCP when the potential reached 2.5 $V_{Ag/AgCl}$ or the transpassive current density reached 1 mA/cm^2.

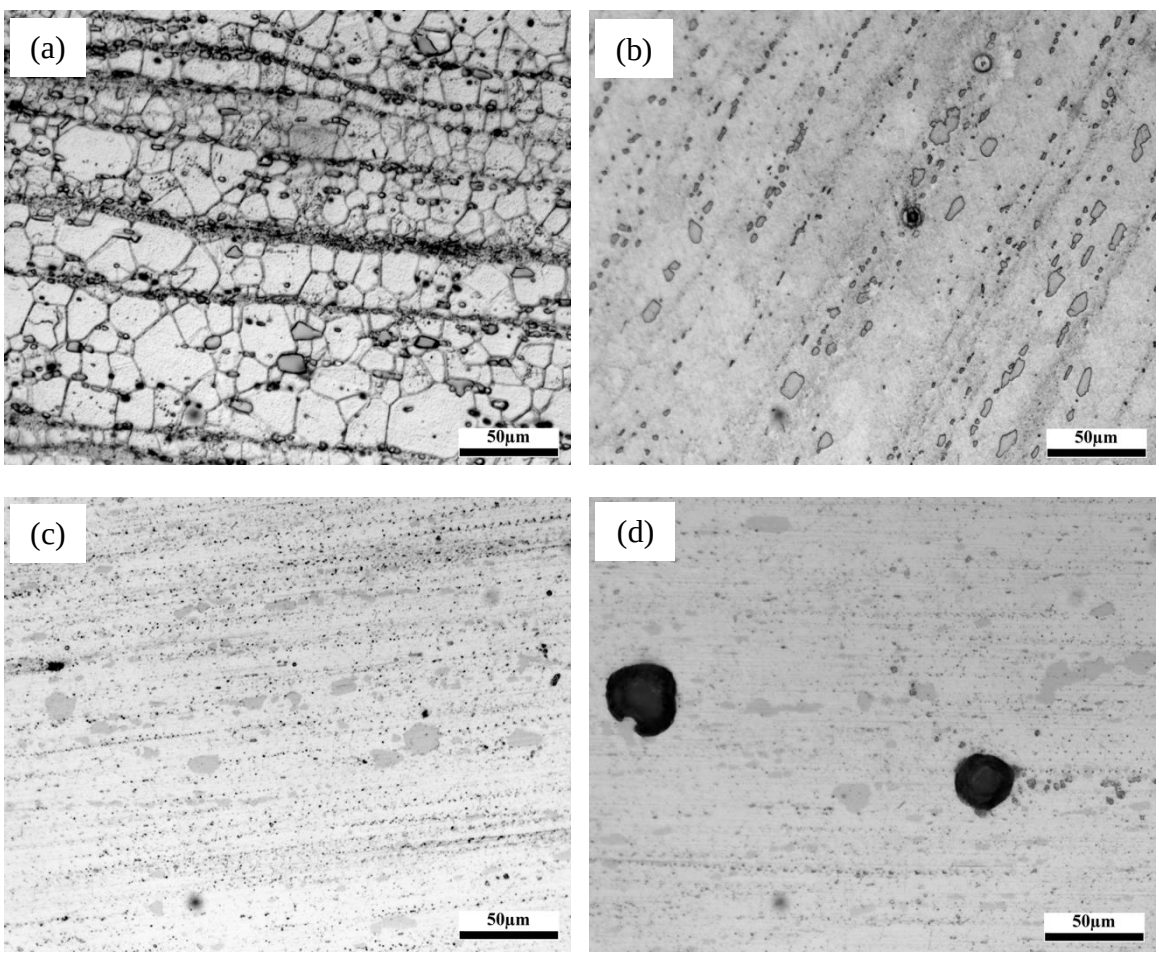

Fig. 1 Microstructure of EV31A AR (a) Non-anodized before cyclic polarization, (b) Non-anodized after cyclic polarization, (c) Anodized before cyclic polarization, (d) Anodized after cyclic polarization

3. RESULTS AND DISCUSSION

3.1 Microstructural Investigation

Figures 1(a) – (d) show microstructure of EV31A AR in non-anodized and anodized conditions. The non-anodized EV31A AR before doing the test (Fig. 1(a)) showed equiaxed fine grains with precipitates. Jakraphan and his co-worker [4] observed the secondary phases as $Mg_{12}Nd$, Mg_3RE and $Mg_{41}Nd_5$. Fine grain size caused by the addition of Zr improve mechanical property and corrosion resistance of EV31A [5, 6]. After the electrochemical test, it could be seen that there was pitting corrosion in secondary phase particles. Jakraphan and co-worker [4] observed that pit initiation of EV31A occurred at the spherical particle which identified as Zr-rich particle. Fig. 1(c) show the anodized EV31A in as-received condition before the electrochemical experiment. Black spots throughout the sample's surface could be noticed. Nemcova and co-workers [7] investigated the anodic film of AZ31 Mg alloy in fluoride/glycerol electrolyte. They found that the film above the Al-Mn particles was porous and non-uniform whereas the film above the matrix was less porous. Compositions of the film form on AZ31 were composed of oxygen and fluorine. Interestingly, the anodic film formed on EV31A AR sample revealed uniform black spots across the sample except on precipitations. This may anticipate that the black spots formed on texture of the sample as seen in Fig. 1(a). In addition, the black spots were also observed at the interface between the matrix and the big irregular-shaped precipitates. These big irregular shaped precipitates were identified as Nd-rich particles as shown in Figs. 2(a) and (b). It should be noted that the compositions of the anodic film of all anodized samples in this work were not examined. Fig. 1(d) shows microstructure of the anodized EV31A AR after cyclic polarization test. Pitting corrosion occurred on the surface of the specimen. Moreover, the density of black spots decreased when the sample exposed to 500 ppm chloride solution.

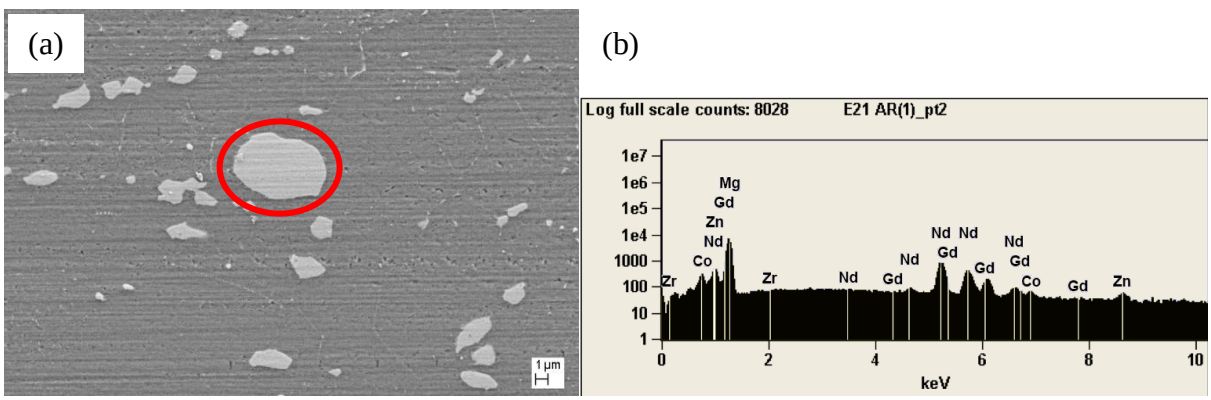

Fig. 2 (a) SEM image of non-anodized EV31A AR before cyclic polarization, (b) Energy dispersive X-ray spectroscopy (EDX) spectrum of the circle particle shown in (a)

Figures 3(a) – (d) show microstructure of EV31A PA specimens. Surface of the non-anodized EV31A PA before the experiment was shown in Fig. 3(a). Texture on the surface as seen in the as-received sample was disappeared, and secondary phase particles located randomly throughout the sample. From the EDX results shown in Figs. 4(a) and (b), these precipitates were identified as Nd-rich particles. After the experiment, localized corrosion also occurred at the center of spherical particles. The anodized EV31A PA sample (Fig. 3(c)) revealed small transparent circles throughout surface included precipitations. Size and pattern of these circles were uniform. Moreover, size of the circles was bigger than the anodized as-received sample. After the cyclic polarization test, localized corrosion was present on surface of the anodized EV31A PA specimen, and a small quantity of transparent circles were left on the surface. Additionally, size of some circles became smaller. Black spots could be noticed.

Figures 5(a) and (b) show microstructure of WE43C in as-received and peak-aged conditions without anodic coating. WE43C AR (Fig. 5(a)) also showed fine grains with texture caused by rolling process as same as EV31A AR. Jakraphan and co-workers [8] examined the secondary phases and identified as $Mg_{12}Nd$, $Mg_{24}Y_5$, Mg_2Y, $Mg_{41}Nd_5$, and Mg_3Gd. In addition, $Mg_{12}RE$, Zr-rich phase, and Zr and Y-rich phase located at grain boundaries. As observed in EV31A, pitting corrosion occurred at spherical Zr-rich particles of WE43C AR [8]. Microstructure of WE43C PA could be seen in Fig. 5(b). Different size and contrasts of grains could be observed. S. Feng and co-workers [9] studied microstructure, mechanical properties and fracture behaviors of sand-cast Mg-4Y-3Nd-1Gd-

0.2Zn-0.5Zr alloy in different thermal conditions. They proposed that different contrasts on grains were present because precipitations were distributed along specific planes with different orientations.

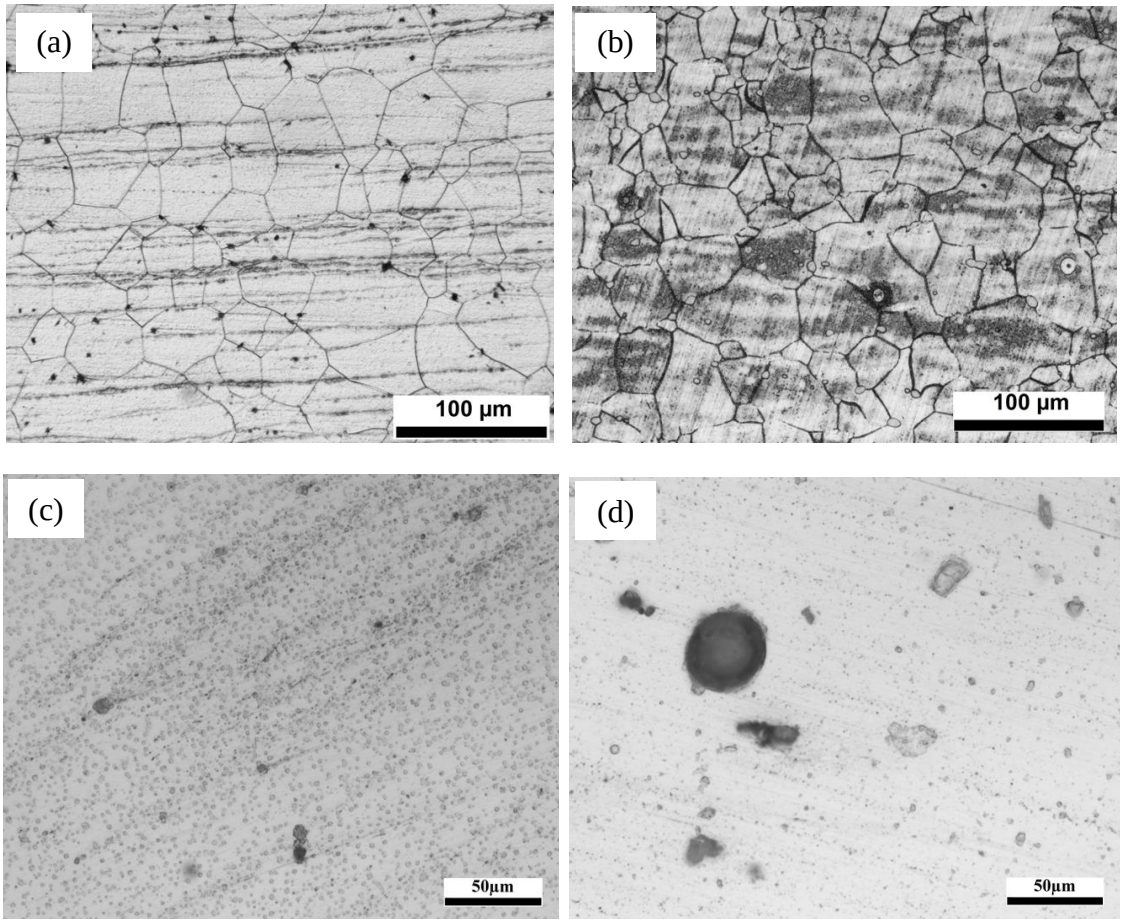

Fig. 3 Microstructure of EV31A PA (a) Non-anodized before cyclic polarization, (b) Non-anodized after cyclic polarization, (c) Anodized before cyclic polarization, (d) Anodized after cyclic polarization

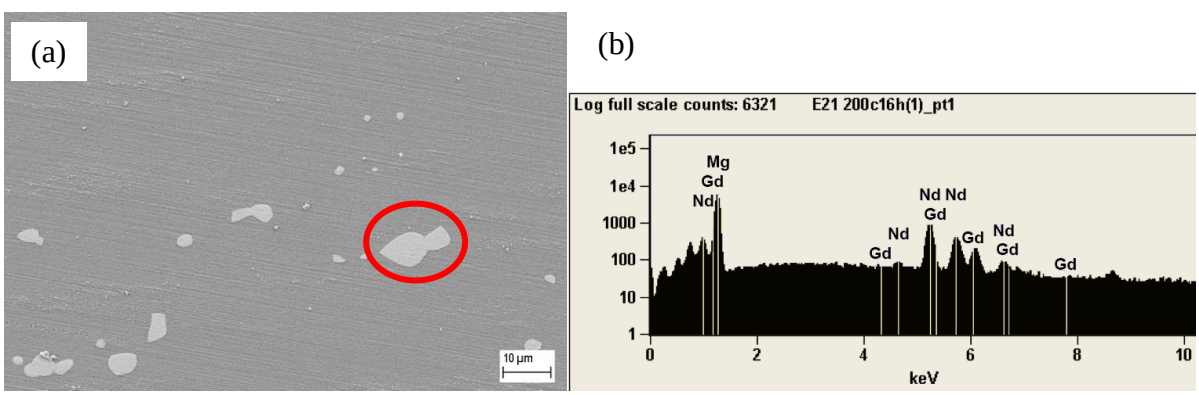

Fig. 4 (a) SEM image of non-anodized EV31A PA before cyclic polarization, (b) EDX spectrum of the circle particle shown in (a)

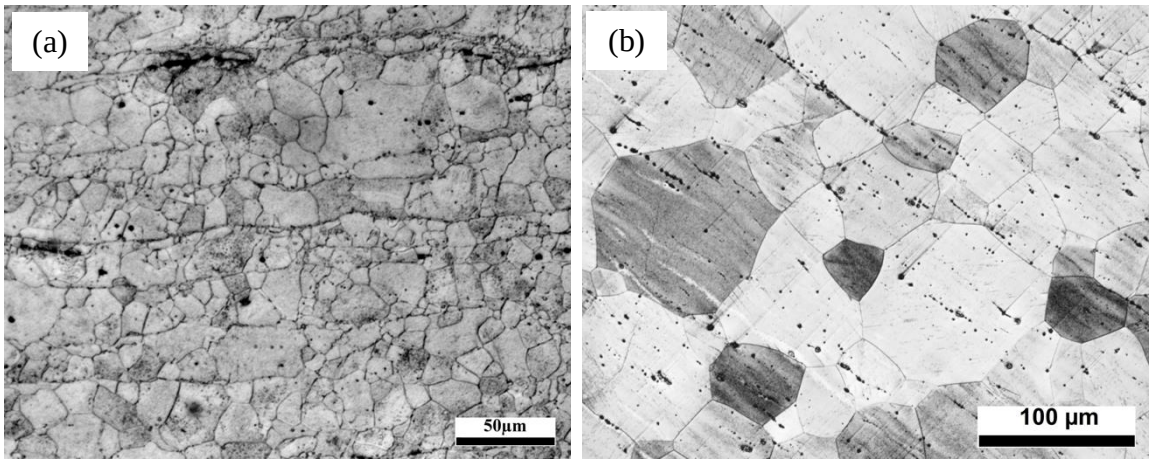

Fig. 5 Microstructure of non-anodized WE43C before cyclic polarization (a) AR, (b) PA

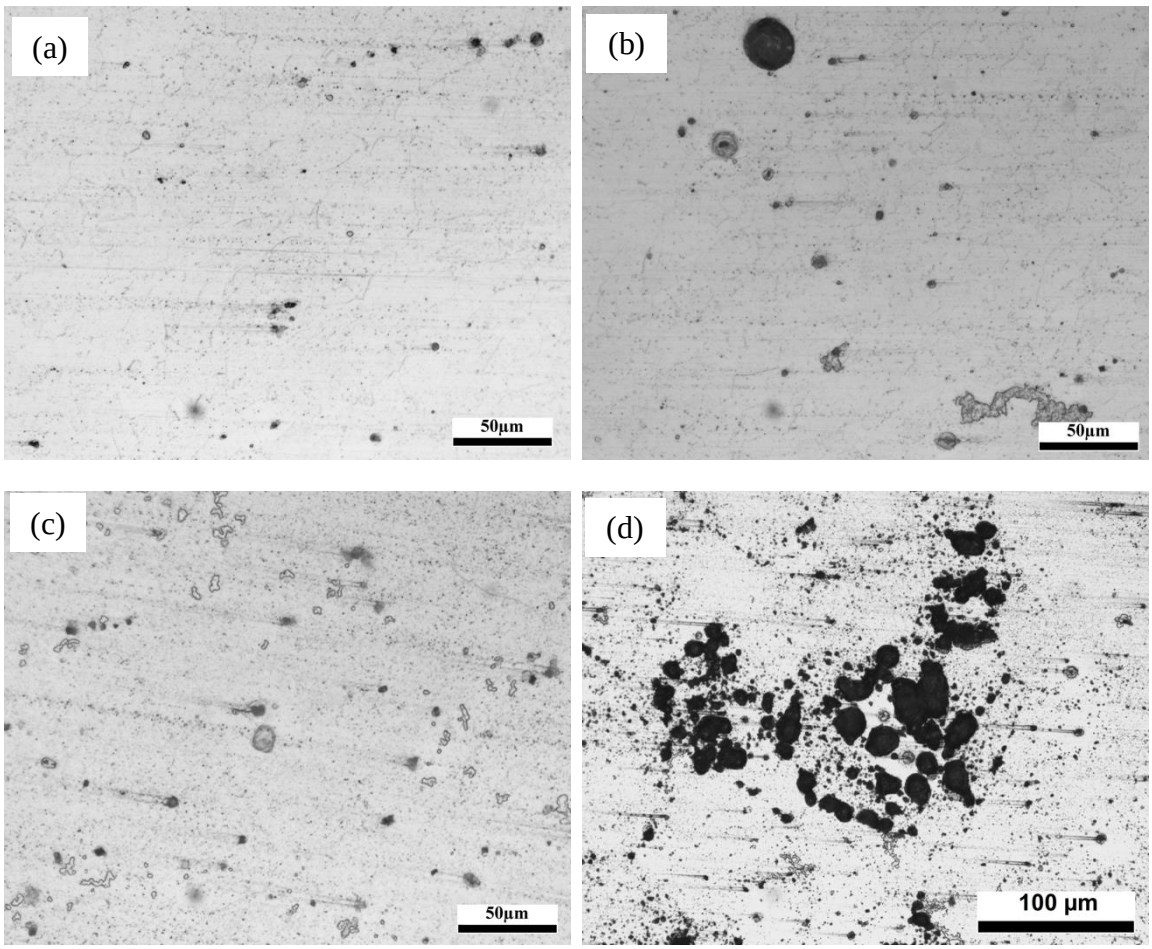

Fig. 6 Microstructure of the anodized WE43C (a) AR before cyclic polarization, (b) AR after cyclic polarization, (c) PA before cyclic polarization, (d) PA after cyclic polarization

Figures 6(a) – (d) show microstructure of anodized WE43C in as-received and peak-aged conditions. Before the test, black spots could be seen throughout surface of both AR and PA conditions, especially along texture of WE43C AR specimen where black spots were dense as shown in Figs. 6(a) and (c). Birss and co-workers [10] studied the characteristics of the oxide film formed on a Mg-based WE43 alloy anodized in silicate solution. They found that the compositions of the oxide film were composed of MgO, $Mg(OH)_2$, MgF_2, and SiO_2. The oxide film

can be divided into 2 layers; the inner barrier and the outer porous oxide film. These pores were larger when high voltages and current densities were applied. After cyclic polarization tests, localized corrosion occurred on both WE43C AR and PA as shown in Figs. 6(b) and (d); however, pit propagation was higher in PA condition. Interestingly, density of black spots on the surface of WE43C AR and PA specimens before and after cyclic polarization tests were not much different.

3.2 Electrochemical Tests (Cyclic Polarization)

Figures 7(a) – (d) show cyclic polarization of EV31A and WE43C samples in different conditions, and Table 1 shows data of Figs. 7(a) – (d). For EV31A AR and PA samples (Figs. 7(a) and (b)), OCPs of the non-anodized conditions were more nobler than the anodized conditions. However, passive current density of both anodized EV31A AR and PA were approximately two times less than the non-anodized condition of the same specimens. This could be anticipated that corrosion resistance of the anodic coated specimens were better than the uncoated specimens. In addition, transpassive potential where passive film breakdown of the anodized EV31A AR and PA were higher than the non-anodized samples. Transpassive potential of EV31A AR and PA in non-anodized condition were 1.61 $V_{Ag/AgCl}$, whereas the anodized EV31A AR and PA had the transpassive potential of 2.37 $V_{Ag/AgCl}$ and 2.41 $V_{Ag/AgCl}$, respectively. Interestingly, anodic coating of EV31A AR did not improve pitting protection potential. Pitting protection potential of both conditions were approximately 1.4 $V_{Ag/AgCl}$. Passive film of the anodized EV31A PA completely breakdown whereas the pitting protection potential of the non-anodized one was 0.57 $V_{Ag/AgCl}$.

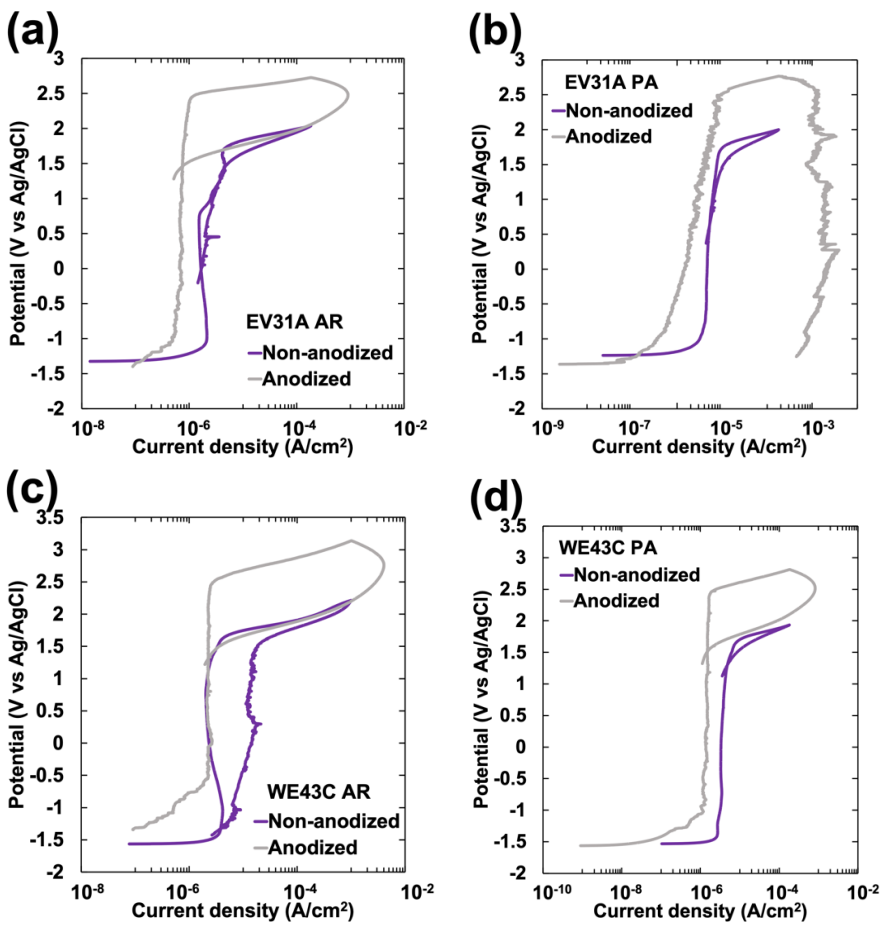

Fig. 7 Cyclic polarization plots of (a) EV31A AR, (b) EV31A PA, (c) WE43C AR, (d) WE43C PA

For WE43C (Figs. 7(c) and (d)), OCP of the coated WE43C AR sample was higher than the uncoated sample. In contrast, the uncoated and coated WE43C PA showed similar OCPs which were -1.53 $V_{Ag/AgCl}$ and -1.56 $V_{Ag/AgCl}$,

respectively. Anodic coating might not affect passive current density or corrosion resistance of the WE43C AR specimen as shown in Fig. 7(c) that passive current density of both conditions were almost the same. On the other hand, passive current density of WE43C PA in anodized condition decreased approximately two times compared to the non-anodized condition. Anodic coating might improve the ability of passive film of WE43C PA. Birss and co-workers [10] found that corrosion resistance of Mg-based WE43 alloy anodized in silicate solution was improved when the inner barrier and outer porous films were thicken, and the area of total pores increased. It could be noticed that transpassive potential and pitting protection potential of the anodic coated WE43C AR and PA samples were improved. Transpassive potential shifted from around 1.5 $V_{Ag/AgCl}$ in non-anodized condition to around 2.4 $V_{Ag/AgCl}$ in anodized condition. Pitting protection potential of WE43C AR shifted from -1.32 $V_{Ag/AgCl}$ to 1.28 $V_{Ag/AgCl}$, and from 1.27 $V_{Ag/AgCl}$ to 1.49 $V_{Ag/AgCl}$ for WE43C PA. Cipriano and co-workers [11] studied the anodization of Mg in KOH electrolyte and the associated surface, degradation, and biological properties for bioresorbable implant applications. Two heat treatment conditions which were anodized condition and anodized and annealed condition. The anodized and annealed Mg had lower current density than the anodized Mg. In addition, passive film of the anodized and annealed Mg was thicker after the long-term immersion test. Localized corrosion was not present. The overall results of cyclic polarization behavior could be summarized that the corrosion resistance of the EV31A AR, WE43C AR and WE43C PA was improved after anodization, whereas no such improvement was observed for the EV31A PA specimens after anodization. The inferior resistance of the anodized EV31A PA specimen could be attributed to the macroscopic defects present in the anodic film. Similar observation was reported by Song et al. [1], who reported the presence of both discontinuous pores, and connected pores. The electrolyte could penetrate and reach the metal/oxide interface only when the pores are interconnected. Since the fraction of the connected pores (or through pores) is significantly less than that of discrete pores, the corrosion resistance was improved by the presence of anodic oxide film. Song et al. called this effect as "blocking effect".

Table 1: Cyclic polarization results of the specimens in Fig. 7

Sample	Anodic condition	OCP (V vs Ag/AgCl)	$E_{Transpassive}$ (V vs Ag/AgCl)	$E_{Cross\ over}$ (V vs Ag/AgCl)	Passive current density ($\mu A/cm^2$)
EV31A AR	Non-anodized	-1.32	1.61	1.43	1.54
	Anodized	-1.37	2.37	1.46	0.72
EV31A PA	Non-anodized	-1.23	1.61	0.57	4.62
	Anodized	-1.36	2.41	-	2.90
WE43C AR	Non-anodized	-1.56	1.55	-1.32	2.12
	Anodized	-1.32	2.40	1.28	2.30
WE43C PA	Non-anodized	-1.53	1.52	1.27	3.34
	Anodized	-1.56	2.35	1.49	1.50

4. CONCLUSION

1) Microstructure of EV31A and WE43C in anodized condition showed spots and circles on surface. They might be pores of the coating layer which could affect the overall corrosion resistance among the anodized samples.
2) Anodic coating improved corrosion resistance of EV31A AR, EV31A PA, and WE43C PA, but corrosion resistance of the coated WE43C AR was not better than the uncoated WE43C AR.
3) Anodic coating improved the resistance of passive film break down of EV31A and WE43C in AR and PA conditions.
4) Pitting protection potential of EV31A AR and PA were not improved by anodic coating. In contrast, anodic coating improved pitting protection potential of both WE43C AR and PA.
Dittus-Boelter correlation:

ACKNOWLEDGEMENT

The support provided by the US Nuclear Regulatory Commission, and Royal Thai Naval Academy are acknowledged.

REFERENCES

[1] Song, G.L. and Shi, Z. Anodization and corrosion of magnesium (Mg) alloys, Corrosion Prevention of Magnesium Alloys, 2013, Woodhead Publishing Limited, Cambridge.

[2] Liyuan, C., Xia, Y., Zhihui, Y., Yunyan, W. and Masazumi, O. Anodizing of magnesium alloy AZ31 in alkaline solutions with silicate under continuous sparking, Corrosion Science, Vol. 50, 2008, pp. 3274-3279.
[3] Wu, C.S., Zhang, Z., Cao, F.H., Zhang, L.J., Zhang, J.Q. and Cao, C.N. Study on the anodizing of AZ31 magnesium alloys in alkaline borate solutions, Applied Surface Science, Vol. 253, 2007, pp 3893-3898.
[4] Ninlachart, J. and Raja, K.S. Threshold chloride concentration for passivity breakdown of Mg-Zn-Gd-Nd-Zr alloy (EV31A) in basic solution, Acta Metallurgica Sinica (English Letters), Vol. 30(4), 2017, pp. 352-366.
[5] Avedesian, M. and Baker, H. ASM speciality handbook: Magnesium and magnesium alloys, 1999, ASM International, Ohio.
[6] Kielbus, A. Microstructure and mechanical properties of Elektron 21 alloy after heat treatment, Journal of Achievements in Materials and Manufacturing Engineering, Vol. 20(1-2) January-February, 2007, pp. 127-130.
[7] Nemcova, A., Galal, O., Skeldon, P., Kubena, I., Smid, M., Briand, E., et al. Film growth and alloy enrichment during anodizing AZ31 magnesium alloy in fluoride/glycerol electrolytes of a range of water contents, Electrochimica Acta, Vol. 219, 2016, pp. 28-37.
[8] Ninlachart, J., Marmiol, Z., Chidambaram, D. and Raja, K.S. Effect of heat treatment conditions on the passivation behavior of WE43C Mg-Y-Nd alloy in chloride containing alkaline environments, Journal of Magnesium and Alloys, Vol. 5, 2017, pp. 147-165.
[9] Zhang, H., Fan, J., Zhang, L., Wu, G., Liu, W., Cui, W., et al. Effect of heat treatment on microstructure, mechanical properties and fracture behaviors of sand-cast Mg-4Y-3Nd-1Gd-0.2Zn-0.5Zr alloy, Materials Science and Engineering A, Vol. 677, 2016, pp. 411-420.
[10] Birss, V., Xia, S., Yue, R. and Rateick, R.G. Jr. Characterization of oxide films formed on Mg-based WE43 alloy using AC/DC anodization in silicate solutions, Journal of The Electrochemical Society, Vol. 151(1), 2004, pp. B1-B10.
[11] Cipriano, A.F., Lin, J., Miller, C., Lin, A., Alcaraz, M.C.C., Soria, P.Jr. et al. Anodization of magnesium for biomedical applications – Processing, characterization, degradation and cytocompatibility, Acta Biomaterialia, Vol. 62, 2017, pp. 397-417.